Selective Expression of RT6 Superfamily in Human Bronchial Epithelial Cells

Enrico Balducci, Koji Horiba, Jiro Usuki, Maryann Park, Victor J. Ferrans, and Joel Moss

Pulmonary-Critical Care Medicine Branch and Pathology Section, National Heart, Lung, and Blood Institute, National Institutes of Health, Bethesda, Maryland

RT6 proteins are glycosylphosphatidylinositol (GPI)-linked alloantigens that are localized to cytotoxic T lymphocytes and that have nicotinamide adenine dinucleotide glycohydrolase and adenosine diphosphate (ADP)-ribosyltransferase activities. In view of the importance of GPI-linked surface proteins in mediating interactions of cells with their milieu, and the varied functions of airway cells in inflammation, we undertook the present study to determine whether human homologues of the RT6 superfamily of ADP-ribosyltransferases (ART) are expressed in pulmonary epithelial cells. We hypothesized that these surface proteins or related family members may be present in cells that interact with inflammatory cells, and that they may thereby be involved in intercellular signaling. Using *in situ* analysis and Northern blot analysis, we identified ART1 messenger RNA (mRNA) in airway epithelial cells. As expected for GPI-anchored proteins, the localization of ART1 at the apical surface of ciliated epithelial cells was demonstrated by staining with polyclonal anti-ART1 antibody, and was confirmed by loss of this immunoreactivity after treatment with phosphatidylinositol-specific phospholipase C (PI-PLC), which selectively cleaves GPI anchors and releases proteins from the plasma membrane. Using *in situ* hybridization with specific ART3 and ART4 oligonucleotides, we also identified two additional members of the RT6 superfamily in epithelial cells. In accord with these findings, we identified ART3 and ART4 mRNAs through reverse transcription–polymerase chain reaction of polyadenine-positive RNA from human trachea. Interestingly, these proteins appeared to be preferentially localized to the airway epithelium. The localized expression of these members of the RT6 superfamily in human pulmonary epithelial cells may reflect a role for them in cell–cell signaling during immune responses within the airway. **Balducci, E., K. Horiba, J. Usuki, M. Park, V. J. Ferrans, and J. Moss. 1999. Selective expression of RT6 superfamily in human bronchial epithelial cells. Am. J. Respir. Cell Mol. Biol. 21:337–346.**

RT6, a glycosylphosphatidylinositol (GPI)-linked protein, is thought to be selectively expressed on the surface of mature peripheral T cells and intraepithelial lymphocytes in rats (1–4). Two allelic variants of RT6, designated RT6.1 and RT6.2, have been found in the rat (5), whereas two copies of the RT6 gene, *Rt6-1* and *Rt6-2* (6), are expressed in the mouse. In experimental animal models, RT6-positive lymphocytes are believed to be determinants of autoimmune diseases (e.g., diabetes mellitus [7], lupus erythematosus [8]), although the role of RT6 in the pathogenesis of these diseases is unclear.

Members of the RT6 family catalyze adenosine diphosphate (ADP)–ribose transfer reactions, using nicotinamide adenine dinucleotide (NAD) as a substrate (9). RT6 proteins in the rat have NAD glycohydrolase (10) and auto-ADP-ribosyltransferase activities (11, 12), but are apparently incapable of ADP-ribosylating exogenous substrates (e.g., histones or simple guanidino compounds such as agmatine). In contrast, mouse Rt6-1 and Rt6-2 ADP-ribosylate simple guanidino compounds and catalyze auto-ADP-ribosylation and NAD hydrolysis (13, 14). The ability of the mouse Rt6 to utilize arginine as an ADP-ribose acceptor reflects the presence of a glutamate at position 207, rather than a glutamine, as is found in rat RT6 (15, 16). In humans, the RT6-related gene has three stop codons in the coding region, and is not expressed (17). Although lacking RT6, human tissues do contain proteins with ADP-ribosyltransferase activity and RT6-related sequences (18–21).

(*Received in original form December 4, 1998 and in revised form March 30, 1999*)

Address correspondence to: Joel Moss, M.D., Ph.D., Pulmonary-Critical Care Medicine Branch, National Heart, Lung and Blood Institute, Building 10/6D05, National Institutes of Health, 10 Center Dr. MSC-1590, Bethesda, MD 20892-1590. E-mail: mossj@fido.nhlbi.nih.gov

Abbreviations: adenosine diphosphate-ribosyltransferase, ADP-RT; nicotinamide adenine dinucleotide, NAD; phosphatidylinositol-specific phospholipase C, PI-PLC; reverse transcription–polymerase chain reaction, RT–PCR.

ADP-ribosyltransferase activity was initially detected in bacterial toxins (e.g., pertussis and cholera toxins), in which it disrupts cellular metabolic or regulatory pathways (22). In eukaryotes, ADP-ribosyltransferase activity has been detected in several avian and mammalian cells and tissues, including turkey erythrocytes (23), chicken heterophils (24), rat liver (25), and several murine cell lines (26). The expression of transferase in mammalian tissues is relatively restricted (9). To date, five ADP-ribosyltransferase family members have been identified in mammalian tissues, and have been termed ADP-ribosyltransferases (ARTs) 1 through 5 (1, 19, 21, 27–29). Transferase clones have been isolated from muscle (ART1) (29), hematopoietic cells (ART1, ART5) (27, 28), spleen (ART4) (21), and testes (ART3) (21). On the basis of primary sequence and biochemical data, some of these proteins (like RT6) appear to be GPI-anchored to the plasma membrane (18). Another transferase, ART5, has been recently cloned from Yac1 cells and, unlike the other ARTs, appears not to be GPI-linked (28). All mammalian ARTs have deduced amino acid sequences that are similar to those of the RT6 proteins of rodents, and are members of the RT6 superfamily (1, 19, 21, 27–29).

In mammalian cells, mono-ADP-ribosylation of proteins has been associated with modifications of key cellular events, such as myocyte differentiation (30) and the function of cytotoxic T lymphocytes (CTLs) (31). Incubation of CTLs with NAD resulted in the ADP-ribosylation of membrane proteins and inhibition of proliferation and cytotoxicity (31). Exposure of CTLs to phosphatidylinositol-specific phospholipase C (PI-PLC) released an NAD: arginine ADP-ribosyltransferase and abolished the inhibitory effect of NAD on CTL function, suggesting that the GPI-linked protein was responsible for this effect. Two proteins present on the surface of CTLs and ADP-ribosylated by the GPI-linked ART1 are lymphocyte function-associated molecule-1 (LFA-1) and p40, a 40-kD protein that inhibits $p56^{lck}$, a T-cell receptor-associated tyrosine kinase (32). An ART cloned from murine CTLs is similar in structure to that identified in a cell line of mouse T-cell (Yac1) lymphoma, and probably represents the murine equivalent of rabbit and human ART1 (27). The latter enzyme, also found in muscle, can ADP-ribosylate the extracellular domain of integrin $\alpha 7\beta 1$ in murine C2C12 muscle cells (33). Given that the transferases from lymphocytes and muscle modify integrins, it appears that transferases may be involved in the regulation of immune responses via cell–cell and cell–matrix interactions.

Airway epithelial cells in the lung play an active role in inflammatory processes by recruiting and interacting with cells such as lymphocytes, monocytes, and macrophages (34). Interaction of these cells with airway epithelium may also be partly responsible for the generation of cytokine- and cell-mediated injury. Because of the potential role of ADP-ribosylation in regulatory interactions, we investigated whether members of the RT6 superfamily are present in pulmonary epithelial cells. As reported here, we demonstrated, through immunohistochemical techniques, *in situ* hybridization, and reverse transcription–polymerase chain reaction (RT–PCR), that human airway epithelial cells express ART1, ART3, and ART4.

Materials and Methods

Preparation of Cells and Tissues

The staining procedures subsequently described were done on human cells obtained by bronchoalveolar lavage (BAL) or bronchial brushing, and in tissue sections of lung. All procedures involving the use of human subjects were approved by the Institutional Review Board of the National Heart, Lung, and Blood Institute. The BAL cells were obtained as described previously from four normal human volunteers (35). Normal human bronchial epithelial cells were obtained from large bronchi and trachea of the same four normal volunteers through bronchoscopy, using a standard cytology brush (Microvasive) (36). The cells were immediately suspended in RPMI-1640 medium at 4°C. After washing twice, cytocentrifuge preparations were made (Cytospin 2; Shandon Instruments, Pittsburgh, PA; 600 rpm, 10 min). Similar preparations were made of the cells recovered by BAL. For immunohistochemical staining, samples of normal lung from two subjects (who died of causes unrelated to pulmonary disease) were fixed in buffered 10% formalin, embedded in paraffin, and sectioned at a thickness of 5 μm. For *in situ* hybridization studies, frozen sections of unfixed human lung and airways were cut in a cryostat at a thickness of 5 μm, using blocks of histologically normal lung tissue obtained from two patients who underwent lobar resection for treatment of lung cancer. The unfixed cells and tissue sections were fixed with ice-cold acetone, air-dried, stored at −80°C, and rehydrated just before use.

Immunoperoxidase Staining

For immunostaining by the peroxidase method, the tissue sections were deparaffinized, hydrated, and incubated for 30 min in 0.3% hydrogen peroxide in methanol to inactivate endogenous peroxidase activity. After washing, the sections were treated with 0.4% pepsin (Sigma Chemical Co., St. Louis, MO) in 0.01 M HCl for 20 min at 37°C. The sections were then washed and incubated with 2% normal goat serum in phosphate-buffered saline (PBS) (0.1 M; pH 7.2) for 20 min at room temperature to block nonspecific binding of the secondary antibody. The sections were then incubated with a rabbit polyclonal antibody against rabbit skeletal muscle ART1 (*see the subsequent discussion*) (1:1,000 dilution) for 18 h at 4°C. The sections were then washed with PBS and processed according to the avidin–biotin–peroxidase complex method, using the Vector Elite Kit (Vector Laboratories, Burlingame, CA) and the Vector VIP kit to produce a purple color at the sites of reactivity. The slides were then counterstained with hematoxylin and mounted.

Immunofluorescence Staining

The sections were treated with blocking serum, washed, and incubated overnight at 4°C with the primary antibody against ART1 (dilution, 1:200). After washing with PBS, the sections were incubated with goat antirabbit immunoglobulin (Ig)G conjugated with fluorescein isothiocyanate (FITC; 1:100 dilution) for 1 h at room temperature. Nuclei were then stained for 20 min at room temperature with 0.1% 4′,6-diamidino-2-phenylindole (DAPI) in PBS. The

preparations were examined with a laser scanning confocal fluorescence microscope (Model TCS4D/DMIRBE; Leica Microsystems Heidelberg GmbH, Heidelberg, Germany) equipped with argon and argon–krypton laser sources.

Immunohistochemical Procedures

For immunohistochemical control procedures, the tissue sections were processed according to protocols in which the primary antibody had been either omitted or replaced by equivalent amounts of normal rabbit IgG. These procedures gave consistently negative results.

Northern Blot Analysis

Polyadenine-positive (poly[A]$^+$) RNA (3 μg; Clontech Laboratories, Palo Alto, CA) was fractionated in a 1% agarose/formaldehyde gel and transferred to nitrocellulose membranes using the Turboblotter system (Schleicher & Schuell, Keene, NH). Membranes were prehybridized in 53 saline–sodium phosphate–ethylenediamine tetraacetic acid (EDTA)/10× Denhardt's solution/50% formamide/2% sodium dodecyl sulfate (SDS)/salmon sperm DNA (100 mg/ml) and were hybridized at 42°C for 18 h in the same solution, containing [^{32}P]deoxyadenosine triphosphate ([^{32}P]dATP)-labeled ART1, ART3, or ART4 transferase complementary DNA (cDNA). Membranes were washed three times in 2× standard saline–citrate (SSC)/0.05% SDS for 10 min at 25°C, and once in 0.5× SSC/0.1% SDS for 30 min at 42°C, before being exposed to X-OMAT AR film (Eastman Kodak, Rochester, NY) for 1 wk.

In Situ Hybridization

Antisense and sense oligonucleotides specific for ART1 (nucleotides [nt] 133–208, 752–827) (18), ART3 (nt 130–205, 670–745) (21), and ART4 (nt 80–154, 620–694) (21) were synthesized with an ABI synthesizer (PE Applied Biosystems, Foster City, CA). Sense probes, complementary to the antisense probes previously described (18, 21), were used as controls in adjacent sections. Antisense and sense probes were labeled with [α-thio-^{35}S]dATP, using terminal deoxynucleotidyl transferase (specific activity $> 1 \times 10^5$ cpm/ng). Cells were prehybridized for 2 h at 42°C in 1 M Tris/HCl (pH 7.5)/5 M NaCl/0.2 M EDTA/50% formamide/10× Denhardt's solution/yeast transfer RNA and 10 mg/ml/salmon sperm DNA at 5 mg/ml/50 mM dithiothreitol (DTT), and were then hybridized overnight at 42°C with the labeled probes in the same buffer containing 50% dextran sulfate. The samples were washed once with 2× SSC at room temperature, once in 2× SSC containing 50% formamide at room temperature, three times in the same buffer at 37°C, and once with distilled water and ethanol before drying and developing with D-19 (1:1) developer (Eastman Kodak).

Antibodies

The anti-ART1 antibody was raised in rabbits, using purified rabbit ART1 (18). The specificity of this antibody was evaluated by immunoblot and dot–blot analyses, using membrane fractions from NMU cells transformed with ART1 cDNA before and after treatment with PI-PLC. The reactivity on dot–blots was greater before than after treatment of NMU membranes with PI-PLC, and was absent with preimmune serum (data not shown). A single 36-kD protein, corresponding in size to that predicted for ART1, reacted on Western blots incubated with anti-ART1 antibody, but not with preimmune serum. The antibody showed some reactivity toward recombinant human ART3 and ART4 in Western blot analyses (Ian Okazaki, unpublished data). The specificity of the antibody for ART1 has not been established in intact cells. For this reason, alternative methods (e.g., *in situ* hybridization, Northern blot analysis, RT–PCR) were used to confirm the expression of ART1. With use of these antibodies, ART1 was localized to the apical surfaces of polarized, ciliated epithelial cells, and was PI-PLC–sensitive, as expected for a GPI-linked protein. To some extent, the antibody may recognize other GPI-linked ARTs in these cells.

Western Blot Analysis, SDS–PAGE, and PI-PLC Treatment

SDS–polyacrylamide gel electrophoresis (PAGE) and Western blotting were performed essentially as described previously (37, 38). Immunoreactivity was detected with an ECL kit (Amersham, Inc., Arlington Heights, IL). Cells were incubated with or without PI-PLC from *Bacillus thurigiensis* (1 U/ml) for 1 h at 30°C before fixation, in order to determine whether the immunoreactivity was specific for a GPI-anchored protein.

Analysis of ART3 and ART4 mRNA by RT-PCR

cDNA synthesis using poly(A)$^+$ RNA from human trachea (Clontech) as a template was done with the Gene AMP RNA PCR Kit (Perkin Elmer, Norwalk, CT) according to the manufacturer's instructions. Briefly, 2 μg of human trachea poly(A)$^+$ RNA was reverse-transcribed, using cloned murine leukemia virus (MuLV) reverse transcriptase (Perkin Elmer) and oligo deoxythymidine$_{12\text{-}18}$ primer in 20 μl of reverse transcriptase buffer (50 mM KCl/10 mM Tris-HCl [pH 8.3]/5 mM $MgCl_2$), and 1 mM each of dATP, deoxyguanosine triphosphate (dGTP), deoxycytosine triphosphate and deoxythymidine triphosphate.

All PCR amplifications (total volume: 100 μl) were done with a cDNA thermocycler (Stratagene, La Jolla, CA) for 35 cycles (95°C for 45 s; 62°, 56°, or 48°C for 45 s; 78°C for 1 min). Taq DNA polymerase (Perkin Elmer) was used with forward (ART3: 5′–ATGAAGACGGGACATTTTGAAATA–3′; ART4: 5′–CAGGTTGCAATTAAAATCGACTTC–3′) and reverse (ART3: 5′–ATAAATCTCTTTGTTGCTCTGTAG–3′; ART4: 5′–ATCATTCTTTCCAAAAGCAGAGT-3′) primers (100 pmol each). A second PCR was done with 2 μl of the first PCR reaction product, with nested forward (ART3: 5′–GCAACCATGATTCTAGTGGAC–3′; ART4: 5′–TCTTTTGATGATCAGTACCAA–3′) and nested reverse (ART3: 5′–ATGGTCATCATTTTAATCAGT–3′; ART4: 5′–TATAGCTATTGCATCTCTCTC–3′) primers (100 pmol each) under conditions identical to those described earlier.

PCR products were evaluated after size-fractionation in 1% agarose gel in 1× Tris–borate–EDTA buffer (85 mM Tris-HCl [pH 8.3]/89 mM boric acid/2 mM EDTA).

Subcloning and DNA Sequencing of ART3 and ART4

The PCR product was directly inserted into PCR TMII vector, using a TA cloning kit from Invitrogen. Competent

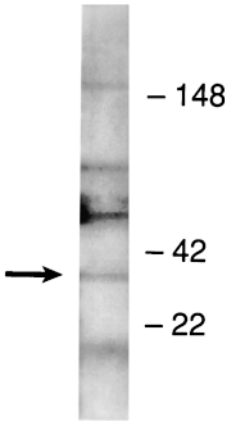

Figure 1. Western blot analysis showing immunoreactivity for ART1 in extract of BAL cells. Proteins (40 μg) in whole cell lysates were separated by SDS–PAGE in a 4–20% gel and transferred to a nitrocellulose membrane, which was incubated with anti-ART1 polyclonal antibody. The positions of the molecular mass markers (kD) are indicated on the right.

Escherichia coli (top 10 F′) were transformed with recombinant plasmid DNA and grown on Luria broth plates containing ampicillin at 100 μg/ml. Plasmid DNA was isolated from *E. coli* with the Qiagen plasmid kit (Qiagen, Carlsbad, CA), and both strands were sequenced with the 7-deaza-dGTP sequencing kit (USB).

Results

Western Blot Analysis

Western blot analysis of cells obtained by BAL revealed an ∼ 40-kD protein that reacted with anti-ART1 antibody (Figure 1), in accord with the presence of a cell-surface membrane-associated ART in alveolar and airway cells.

Immunohistochemical Observations

Study of human lung sections stained with the anti-ART1 antibody showed localization of immunoreactivity in epithelial cells lining the airway (Figure 2). Confirming these results, ciliated (Figures 3A and 3B) and intermediate

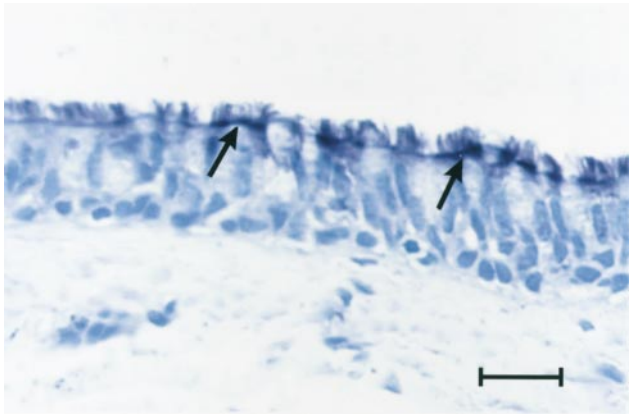

Figure 2. Immunolocalization of ART1 in section of human lung stained with the immunoperoxidase method. Immunoreactivity (*arrows*) is limited to the apical surfaces of epithelial cells lining the airway. Immunoreactivity was not detected in control sections stained with preimmune serum or with only the secondary antibody. Nuclei are counterstained with hematoxylin. *Bar* = 100 μm.

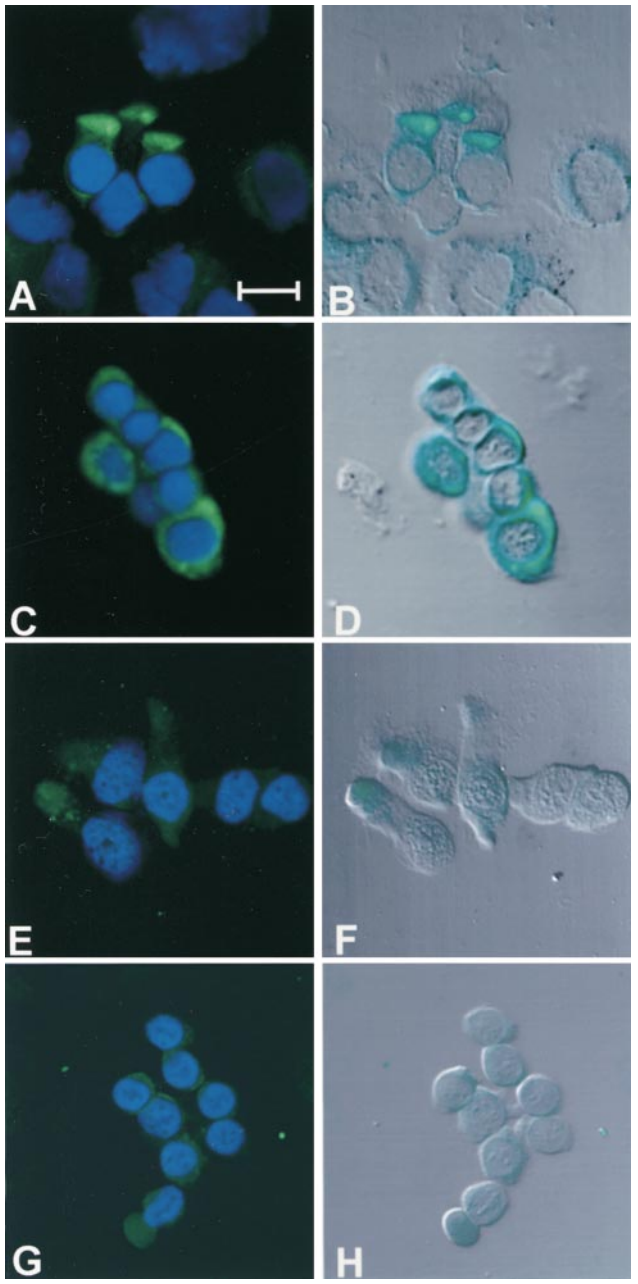

Figure 3. Effect of treatment with PI-PLC on the reactivity of pulmonary ciliated and intermediate epithelial cells (obtained by BAL) for ART1. Control (*A* through *D*) and PI-PLC–treated (*E* through *H*) cells were reacted with anti-ART1 primary antibody followed by FITC-conjugated secondary antibody; nuclei were then counterstained with DAPI. Scale bar for all panels = 10 μm. The panels on the left (*A*, *C*, *E*, and *G*) show confocal microscopic images, in which immunoreactivity is shown in *green* and nuclear structure in *blue.* The panels on the right (*B*, *D*, *F*, and *H*) show the corresponding images created by superimposition of the green fluorescence signal (ART1) on a Nomarski differential interference contrast image to demonstrate the morphology of the cells. (*A* and *B*) Untreated ciliated epithelial cells show immunoreactivity in their apical portions. (*C* and *D*) Untreated intermediate cells show reactivity along their surfaces. (*E* through *H*) Pretreatment with PI-PLC caused a marked reduction in the immunoreactivity of ciliated (*E* and *F*) and intermediate (*G* and *H*) epithelial cells for ART1.

(Figures 3C and 3D) epithelial cells displayed very intense fluorescence after incubation with anti-ART1 antibodies. In contrast, neither macrophages nor lymphocytes reacted with anti-ART1 antibody (data not shown). The apical localization of the immunoreactivity in polarized cells (Figure 3A), and the diffuse surface localization in nonpolarized cells (Figure 3C), are consistent with the presence of a GPI-anchored protein. As noted in MATERIALS AND METHODS, the antibodies did recognize other ARTs, and conceivably, these GPI-linked proteins contribute to the immunoreactivity observed in these areas. After incubation of epithelial cells with PI-PLC, an enzyme that specifically cleaves GPI anchors, the immunofluorescence observed with anti-ART1 antibodies was significantly reduced on the apical surface of ciliated epithelial cells (Figures 3E and 3F) and, overall, on the surface of intermediate epithelial cells (Figures 3G and 3H). Treatment with PI-PLC did not affect the localization of caveolin, an integral membrane protein (39), as determined with anticaveolin antibody (data not shown). Alveolar macrophages showed no reactivity with the ART1 antibody.

Northern Blot Analysis and *In Situ* Localization of ART1 mRNA

The presence of ART1 mRNA was evaluated through Northern blot analysis. A 1.6-kb transcript was observed in poly(A)$^+$ RNA from human trachea (Figure 4, *lane T*), but not from total lung poly(A)$^+$ RNA (Figure 4, *lane L*). These findings are compatible with the proposal that ART1 mRNA is preferentially expressed in the airway. The low signal intensity may reflect the fact that transferases are expressed at low levels in mammalian tissues. In cardiac or skeletal muscle, which are good sources of ART1, a $>$ 200,000-fold enrichment was necessary to obtain sufficiently pure enzyme for sequencing (29). Using *in situ* hybridization, we found that ART1 mRNA was localized to the epithelial layer of the airways in sections of human lung (Figures 5A and 5B). Among cells obtained by BAL and bronchial brushing, ciliated (Figures 5C and 5D) and intermediate (Figures 5E and 5F) epithelial cells reacted strongly with the antisense ART1 oligonucleotides. ART1 mRNA was not detected in macrophages (Figures 5G and 5H).

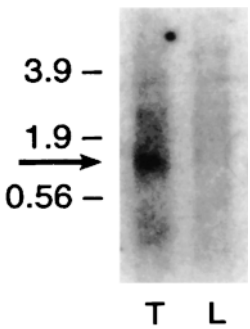

Figure 4. Hybridization of human tracheal poly(A)$^+$ RNA with ART1 cDNA. Poly(A)$^+$ RNA was separated by electrophoresis in 1% formaldehyde–agarose gel (3 μg/lane), transferred to a nitrocellulose membrane, and hybridized with full-length ART1 cDNA labeled with [^{32}P]dATP. Autoradiograms were exposed for 1 wk at −80°C. ART1 cDNA hybridized specifically with a 1.6-kb band from human tracheal poly(A)$^+$ RNA (*lane T*); no hybridization with human lung poly(A)$^+$ RNA (*lane L*) was detected. The sizes (kb) of the standards are indicated on the left.

Detection of ART3 and ART4 mRNA in Human Lung by Antisense Hybridization

Hybridization with antisense probes clearly demonstrated ART3 and ART4 mRNA in the epithelial cell layer in sections of human lung (Figures 6A and 7A). With control ART3 and ART4 sense probes, significantly less hybridization was observed (Figures 6B and 7B). Hybridization with antisense and sense ART oligonucleotides of cells obtained from BAL and brushing revealed that ciliated (Figures 6C and 6D) and intermediate (Figures 6E and 6F) epithelial cells contained ART3 mRNA. Macrophages did not hybridize specifically with the antisense probes (Figures 6G and 6H). As shown in Figures 7A through 7H, results of *in situ* hybridization studies with ART4 were similar to those obtained with ART3.

Detection of ART3 and ART4 by RT–PCR in Human Tracheal Cells

To confirm the presence of ART3 and ART4 mRNAs in epithelial cells, poly(A)$^+$ RNA from human trachea was subjected to RT–PCR with primers based on sequences at the 5′- and 3′- ends of the coding regions (full length), followed by amplification with nested primers. The sizes of the ART3 and ART4 PCR products (1,100 and 800 bp, respectively) were consistent with those predicted from the published sequences (Figure 8). In view of the problems inherent in the identification of low levels of RNAs with RT–PCR, the PCR products were subcloned and sequenced. The sequences of the PCR products were identical to those reported for ART3 and ART4 (data not shown).

Discussion

The results of the present study show for the first time the presence of three members (ART1, ART3, and ART4) of the RT6 superfamily of proteins in human bronchial epithelial cells. These proteins were detected and localized in the epithelial cells through the following techniques: (*1*) SDS–PAGE and Western blot analyses, using whole lysates of bronchial epithelial cells as substrate and an ART1-specific polyclonal antibody; (*2*) immunoperoxidase staining of sections of lung; (*3*) indirect immunofluorescence staining of bronchial epithelial cells before and after PI-PLC treatment; (*4*) hybridization of poly(A)$^+$ RNA from human trachea and lung with ART1 cDNA; (*5*) localization of ART1, ART3, and ART4 through *in situ* hybridization with specific antisense and sense oligonucleotides as reactants and lung sections or bronchial epithelial cells as substrates; and (*6*) RT–PCR methods, using human tracheal poly(A)$^+$ RNA and "full-length" or selected nested ART3 and ART4 forward and reverse primers.

The RT6 superfamily consists of a group of structurally related GPI-linked proteins that have a high degree of sequence identity and which possess ADP-ribosyltransferase/NAD glycohydrolase activity. The RT6 proteins are alloantigens, the expression of which is believed to be restricted to T cells and intraepithelial lymphocytes (4, 40, 41). ART1 is expressed in skeletal (29) and cardiac muscle (18), and in lymphocytes (27). Other members of this su-

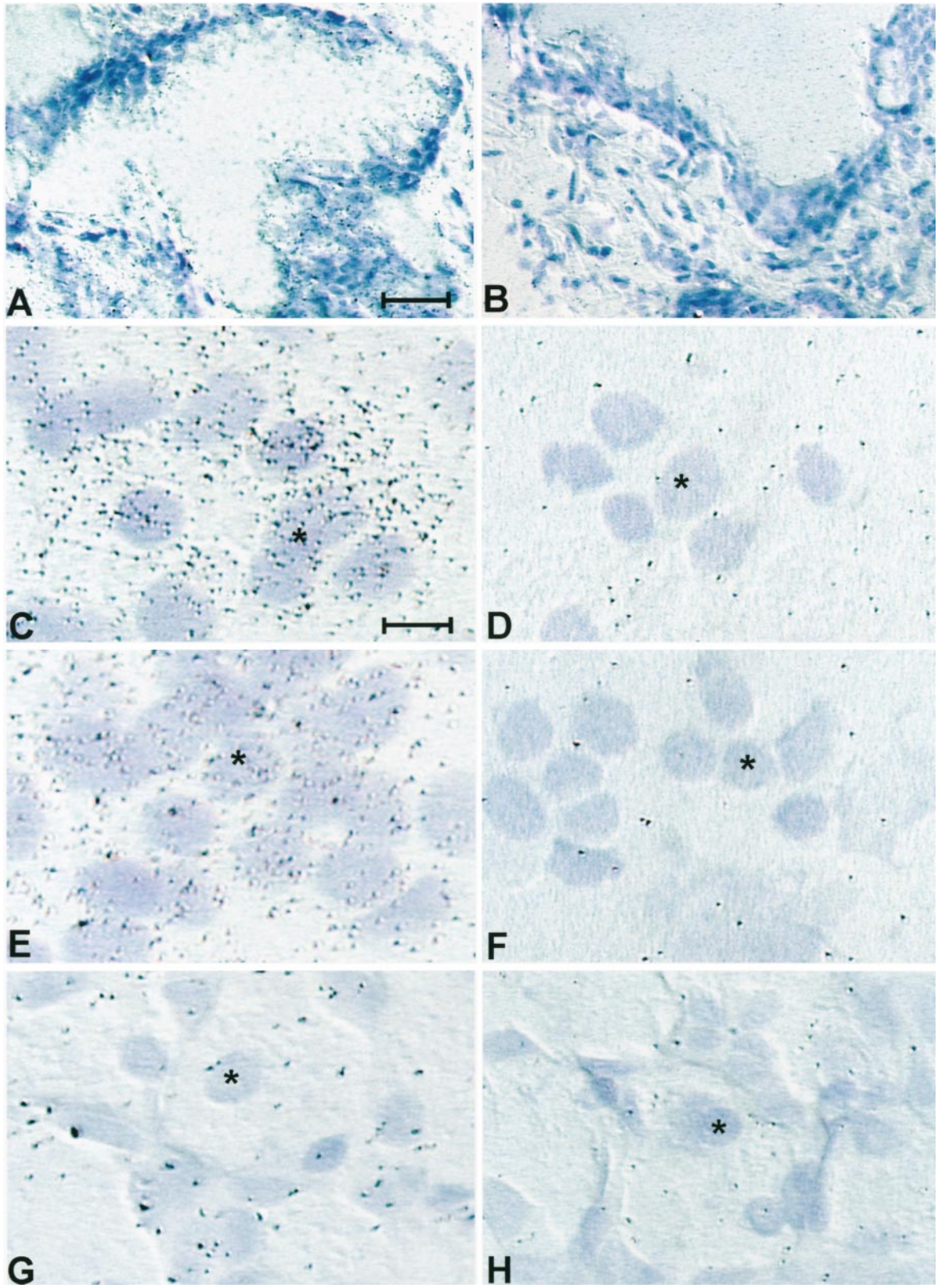

Figure 5. Localization of ART1 mRNA through *in situ* hybridization, as shown by Nomarski differential interference contrast optics. Lung sections (*A* and *B*) and cells from bronchial brushings (*C* through *H*) were hybridized with ^{35}S-labeled ART1 antisense (*A*, *C*, *E*, and *G*) or sense (*B*, *D*, *F*, and *H*) oligonucleotides. Autoradiography showed strong hybridization with ciliated (*asterisk* in *C* and *D*) and intermediate (*asterisk* in *E* and *F*) epithelial cells, but not with alveolar macrophages (*asterisk* in *G* and *H*). The intermediate epithelial cells can be distinguished from macrophages by their more elongated shape and swollen size, as compared with the larger size, more abundant cytoplasm, and absence of cytoplasmic granules in macrophages. Parallel controls incubated with sense probes were negative. Scale bar for *A* and *B* = 100 μm; scale bar for *C* through *H* = 10 μm.

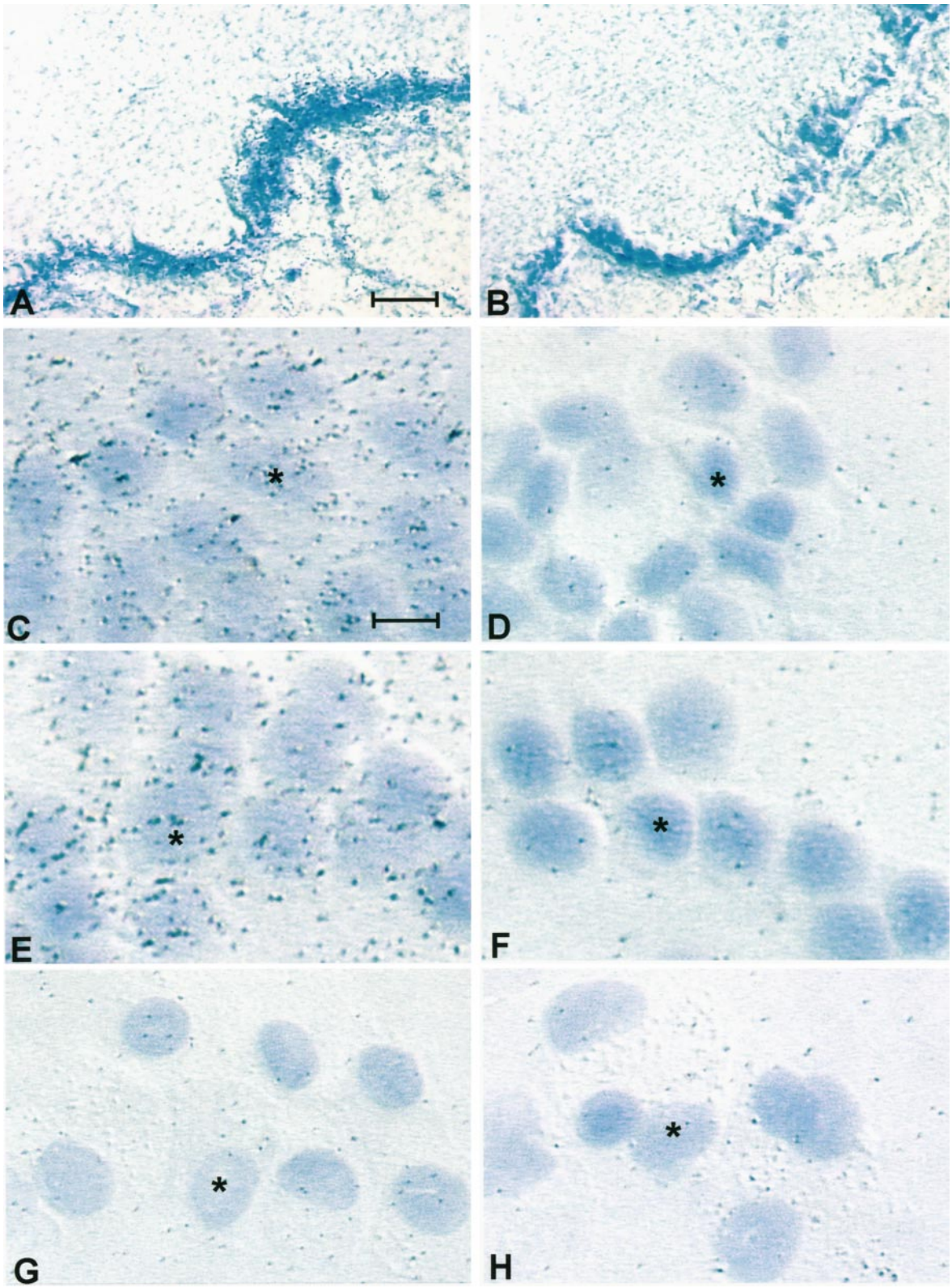

Figure 6. Localization of ART3 mRNA through *in situ* hybridization. As in Figure 5, lung sections (*A* and *B*) and cells from bronchial brushings (*C* through *H*) were hybridized with ^{35}S-labeled ART3 oligonucleotides. Antisense probes (*A*, *C*, *E*, and *G*), but not sense probes (*B*, *D*, *F*, and *H*), showed localization to airway lining cells, including ciliated (*asterisk* in *C* and *D*) and intermediate (*asterisk* in *E* and *F*) epithelial cells. There was no significant reaction in alveolar macrophages (*asterisk* in *G* and *H*). Hybridization was not detected with the sense probe (*B*, *D*, *F*, and *H*). Scale bar for *A* and *B* = 100 μm; scale bar for *C* through *H* = 10 μm.

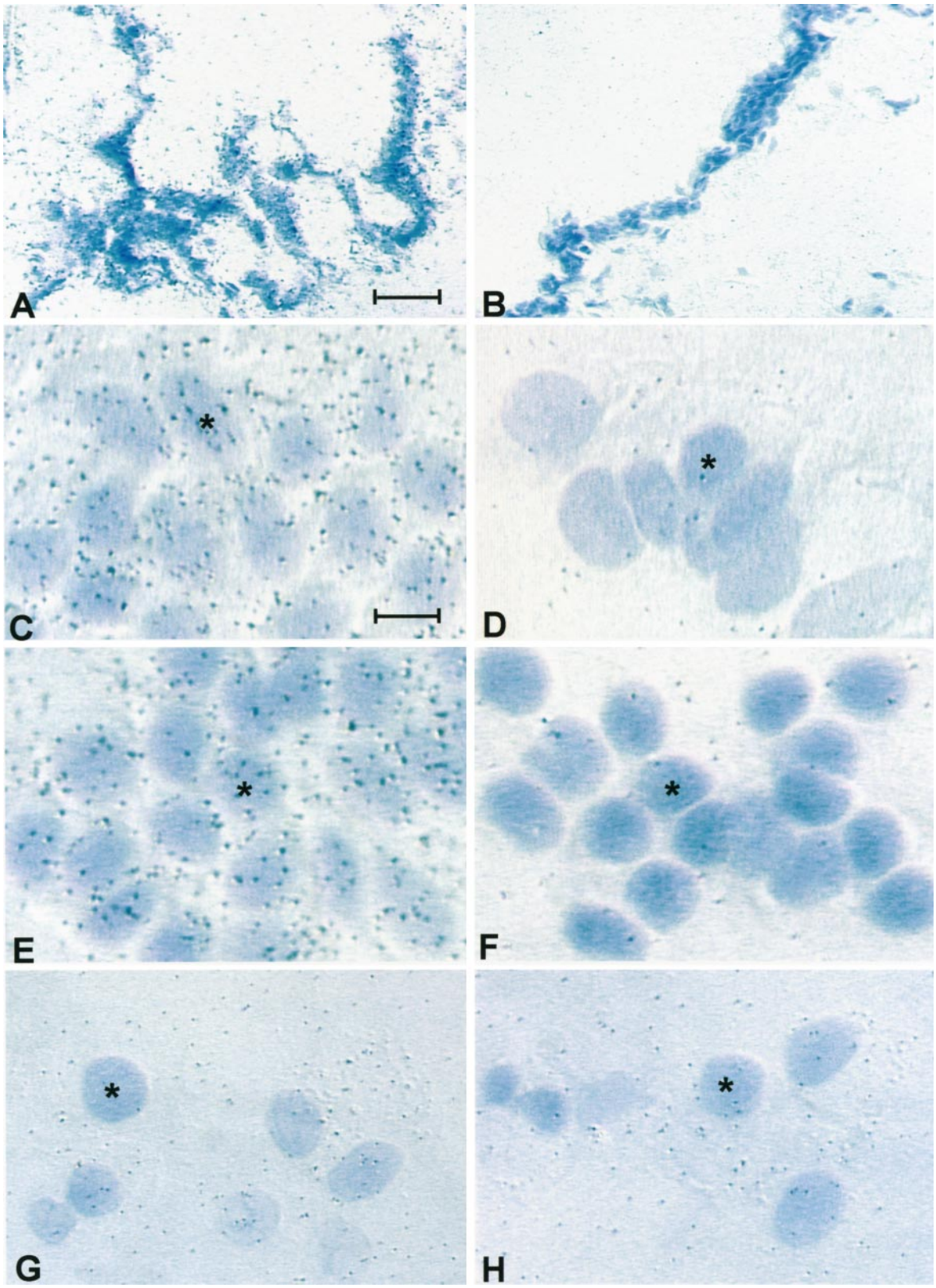

Figure 7. Localization of ART4 mRNA through *in situ* hybridization, as shown by Nomarski differential interference contrast optics. As in Figure 5, lung sections (*A* and *B*) and cells from bronchial brushings (*C* through *H*) were hybridized with antisense (*A*, *C*, *E*, and *G*) or sense (*B*, *D*, *F*, and *H*) oligonucleotides specific for ART4 mRNA. Antisense probes hybridized with airway lining cells (*A*) and with ciliated (*asterisk* in *C* and *D*) and intermediate (*asterisk* in *E* and *F*) epithelial cells; alveolar macrophages (*asterisk* in *G* and *H*) were negative. No hybridization with sense probes was detected. Scale bar for *A* and *B* = 100 μm; scale bar for *C* through *H* = 10 μm.

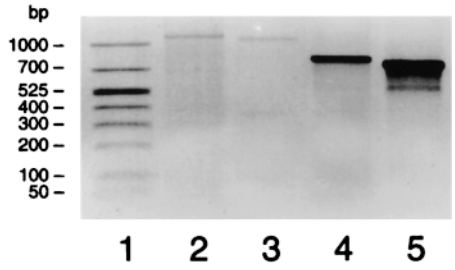

Figure 8. Detection of ART3 and ART4 mRNA in human tracheal poly(A)$^+$ RNA. Samples (2 μg) of poly(A)$^+$ RNA were used for RT–PCR with "full-length" (*lanes 2 and 4*) and nested ART3 and ART4 primers (*lanes 3 and 5*). The experiment was repeated twice with similar results. The sizes (bp) of the oligonucleotide standards are shown on the left.

perfamily of enzymes, ART3 and ART4, appear to have similarly limited patterns of expression, having recently been found in testis and spleen (21). We have now found that in the lung, there is a constitutive and restricted cellular expression of three RT6 family members: ART1, ART3, and ART4. In human airways, the presence of these proteins and/or their mRNAs was demonstrated in ciliated and intermediate bronchial epithelial cells.

Expression in the same cells of structurally related proteins that catalyze the same reactions would seem redundant. The presence of multiple ART proteins in ciliated and intermediate epithelial cells may reflect different roles and substrate specificities for these enzymes.

That all three enzymes are selectively expressed in airway epithelial cells is consistent with the possibility that ARTs may have roles in airway inflammatory responses. In inflammation, bronchial epithelial cells interact with neighboring cells as well as with cells in the airway lumen. These interactions are important not only for restricting access to the interstitium, but also for influencing the composition and activity of the cellular population of the airway lumen. Participation of airway epithelial cells in inflammatory reactions can occur through several mechanisms. The cells can be activated directly by foreign substances or microorganisms, or indirectly by cytokines or other proteins (e.g., adhesion molecules) released from alveolar macrophages or adjacent epithelial cells (42). The GPI-anchored transferases of these cells, which line the airway lumen, may behave as adhesion molecules and thereby recruit inflammatory cells to the site, or may serve as receptors for luminal proteins. By virtue of their transferase activity, airway epithelial cells may modify the activity of molecules on the surfaces of neighboring cells (43, 44).

The normal airway epithelium serves as a barrier to the attachment of and invasion by microbes (45). Some microorganisms have, however, developed mechanisms to invade the respiratory epithelium by using cell-surface molecules as receptors (46). Respiratory pathogens or their toxins might interact with GPI-linked ARTs expressed on the surface of respiratory epithelial cells to gain entry into the epithelium. Indeed, it has been reported that a GPI-linked protein serves as a receptor for aerolysin toxin (47).

ADP-ribosyltransferases can catalyze auto-ADP-ribosylation as well as ADP-ribosylation of membrane surface proteins. In this and related reactions, transferases utilize extracellular NAD, as do the ADP-ribosyl cyclases, such as CD38 (48) and other NAD-glycohydrolases, which are ubiquitously expressed by inflammatory cells such as lymphocytes and macrophages. For these reactions to be physiologically relevant, a supply of extracellular NAD is needed at the cell surface. NAD might be released into the airway during inflammation, cell lysis, and apoptosis. Thus, NAD produced by target cells may be transiently and locally available for ADP-ribosylation. Because the environment of airway epithelial cells is crucial for immune responses in the lung, the finding that epithelial cells express GPI-linked proteins of the RT6 superfamily could be helpful in understanding how these cells interact with inflammatory cells and pathogens in the airway.

Acknowledgments: The authors thank Dr. Martha Vaughan and Dr. Ian J. Okazaki for critical review of the manuscript, and C. Jane Bell for expert secretarial assistance.

References

1. Koch, F., F. Haag, A. Kashan, and H. G. Thiele. 1990. Primary structure of rat RT6.2, a nonglycosylated phosphatidylinositol-linked surface marker of postthymic T cells. *Proc. Natl. Acad. Sci. USA* 87:964–967.
2. Thiele, H.-G., F. Koch, and A. Kashan, 1987. Postnatal distribution profiles of Thy-1+ and RT6+ cells in peripheral lymph nodes of DA rats. *Transplant. Proc.* 19:3157–3160.
3. Crisà, L., P. Sarkar, D. J. Waite, F. Haag, F. Koch-Nolte, T. V. Rajan, J. P. Mordes, E. S. Handler, H.-G. Thiele, A. A. Rossini, and D. L. Greiner. 1993. An RT6^a gene is transcribed and translated in lymphopenic diabetes-prone BB rats. *Diabetes* 42:688–695.
4. Fangman, J., R. Schwinzer, M. Winkler, and K. Wonigeit. 1990. Expression of RT6 alloantigens and the T-cell receptor on intestinal intraepithelial lymphocytes of the rat. *Transplant. Proc.* 22:2543–2544.
5. Haag, F., F. Koch, and H.-G. Thiele. 1990. Polymorphism between rat T-cell alloantigens RT6.1 and RT6.2 is based on multiple amino acid substitutions. *Transplant. Proc.* 22:2541–2542.
6. Prochazka, M., H.R. Gaskins, E. H. Leiter, F. Koch-Nolte, F. Haag, and H.-G. Thiele. 1991. Chromosomal localization, DNA polymorphism, and expression of Rt-6, the mouse homologue of rat T-lymphocyte differentiation marker RT6. *Immunogenetics* 33:152–156.
7. Greiner, D. L., E. S. Handler, K. Nakanko, J. P. Mordes, and A. A. Rossini. 1986. Absence of the RT6 T cell subset in diabetes-prone BB/W rats. *J. Immunol.* 136:148–151.
8. Koch-Nolte, F., J. Klein, C. Hollmann, M. Kuhl, F. Haag, R. Gaskins, E. Leiter, and H. G. Thiele. 1995. Defects in the structure and expression of the genes for the cell marker Rt6 in NZW and (NZB XNZW) F1 mice. *Int. Immunol.* 7:883–890.
9. Okazaki, I. J., and J. Moss. 1996. Mono ADP-ribosylation: a reversible post-translational modification of proteins. *Adv. Pharmacol.* 35:247–280.
10. Takada, T., K. Iida, and J. Moss. 1994. Expression of NAD glycohydrolase activity by rat mammary adenocarcinoma cells transformed with rat T-cell alloantigen RT6.2. *J. Biol. Chem.* 269:9420–9423.
11. Rigby, M. R., R. Bortell, L. A. Stevens, J. Moss, T. Kanaitsuka, H. Shigeta, J. P. Mordes, D. L. Greiner, and A. A. Rossini. 1996. Rat RT6.2 and mouse Rt6 locus 1 are NAD+:arginine ADP-ribosyltransferases with auto-ADP–ribosylation activity. *J. Immunol.* 156:4259–4265.
12. Haag, F., V. Andersen, S. Karsten, F. Koch-Nolte, and H.-G. Thiele. 1995. Both allelic forms of the rat T cell differentiation marker RT6 display nicotinamide adenine dinucleotide (NAD)-glycohydrolase activity, yet only RT6.2 is capable of automodification upon incubation with NAD. *Eur. J. Immunol.* 25:2355–2361.
13. Koch-Nolte, F., D. Petersen, S. Balasubramanian, F. Haag, D. Kahlke, T. Willer, R. Kastelein, F. Bazan, and H.-G. Thiele. 1996. Mouse T cell membrane proteins Rt6-1 and Rt6-2 are arginine/protein mono(AD-ribosyl)transferases and share secondary structure motifs with ADP-ribosylating bacterial toxins. *J. Biol. Chem.* 271:7686–7693.
14. Moss, J., L. A. Stevens, E. Cavanaugh, I. J. Okazaki, R. Bortell, T. Kanaitsuka, J. P. Mordes, D. L. Greiner, and A. A. Rossini. 1997. Characterization of mouse Rt6.1 NAD:arginine ADP-ribosyltransferase. *J. Biol. Chem.* 272:4342–4346.
15. Maehama, T., S.-I. Hoshino, and T. Katada. 1996. Increase in ADP-ribosyltransferase activity of rat T-lymphocyte alloantigen RT6.1 by a single amino acid mutation. *FEBS Lett.* 388:189–191.
16. Hara, N., M. Tsuchiya, and M. Shimoyama. 1996. Glutamic acid 207 in ro-

dent T-cell RT6 antigens is essential for arginine-specific ADP-ribosylation. *J. Biol. Chem.* 271:29552– 29555.
17. Haag, F., F. Koch-Nolte, M. Kuhl, S. Lorenzen, and H.-G. Thiele. 1994. Premature stop codons inactivate the RT6 genes of the human and chimpanzee species. *J. Mol. Biol.* 243:537–546.
18. Okazaki, I. J., A. Zolkiewska, M. S. Nightingale, and J. Moss. 1994. Immunological and structural conservation of mammalian skeletal muscle glycosylphosphatidylinositol-linked ADP-ribosyltransferases. *Biochemistry* 33: 12828–12836.
19. Levy, I., Y.-Q. Wu, N. Roeckel, F. Bulle, A. Pawlak, S. Siegrist, M.G. Mattèi, and G. Guellaën. 1996. Human testis specifically expresses a homologue of the rodent T lymphocytes RT6 mRNA. *FEBS Lett.* 382:276–280.
20. Donnelly, L. E., N. B. Rendell, S. Murray, J. R. Allport, G. Lo, P. Kefalas, G. W. Taylor, and J. MacDermot. 1996. Arginine-specific mono(ADP-ribosyl)transferase activity on the surface of human polymorphonuclear neutrophil leucocytes. *Biochem. J.* 315:635–641.
21. Koch-Nolte, F., F. Haag, R. Braren, M. Kühl, J. Hoovers, S. Balasubramanian, F. Bazan, and H.-G. Thiele. 1997. Two novel human members of an emerging mammalian gene family related to mono-ADP-ribosylating bacterial toxins. *Genomics* 39:370–376.
22. Moss, J., and M. Vaughan. 1988. ADP-ribosylation of guanyl nucleotide-binding regulatory proteins by bacterial toxins. *Adv. Enzymol. Relat. Areas Mol. Biol.* 61:303–379.
23. Moss, J., S. J. Stanley, and P.A. Watkins. 1980. Isolation and properties of an NAD and guanidine-dependent ADP-ribosyltransferase from turkey erythrocytes. *J. Biol. Chem.* 255:5838–5840.
24. Mishima, K., M. Terashima, S. Ohara, K. Yamada, K. Imai, and M. Shimoyama. 1991. Arginine-specific ADP-ribosyltransferase and its acceptor protein p33 in chicken polymorphonuclear cells: co-localization in the cell granules, partial characterization, and *in situ* mono (ADP-ribosylation). *J. Biochem.* 110:338–394.
25. Moss, J., and S. J. Stanley. 1981. Amino acid-specific ADP-ribosylation: identification of an arginine-dependent ADP-ribosyltransferase in rat liver. *J. Biol. Chem.* 256:7830–7833.
26. Soman, G., A. Haregewoin, R.C. Hom, and R.W. Finberg. 1991. Guanidine group specific ADP-ribosyltransferase activity in murine cells. *Biochem. Biophys. Res. Commun.* 176:301–308.
27. Okazaki, I. J., H.-J. Kim, H. G. McElvaney, E. Lesma, and J. Moss. 1996. Molecular characterization of a glycosylphosphatidylinositol-linked ADP-ribosyltransferase from lymphocytes. *Blood* 88:915–921.
28. Okazaki, I. J., H.-J. Kim, and J. Moss. 1996. Cloning and characterization of a novel membrane associated lymphocyte NAD:arginine ADP-ribosyltransferase. *J. Biol. Chem.* 271:22052–22057.
29. Zolkiewska, A., M. S. Nightingale, and J. Moss. 1992. Molecular characterization of NAD:arginine ADP-ribosyltransferase from rabbit skeletal muscle. *Proc. Natl. Acad. Sci. USA* 89:11352–11356.
30. Kharadia, S. V., T. W. Huiatt, H.-Y. Huang, J. E. Peterson, and D. J. Graves. 1992. Effect of an arginine-specific ADP-ribosyltransferase inhibitor on differentiation of embryonic chick skeletal muscle cells in culture. *Exp. Cell. Res.* 201:33–42.
31. Wang, J., E. Nemoto, A. Y. Kots, H. R. Kaslow, and G. Dennert. 1994. Regulation of cytotoxic T cells by ecto-nicotinamide adenine dinucleotide (NAD) correlates with cell surface GPI-anchored/arginine ADP-ribosyltransferase. *J. Immunol.* 153:4048–4058.
32. Nemoto, E., Y. Yu, and G. Dennert. 1996. Cell surface ADP-ribosyltransferase regulates lymphocyte function-associated molecule-1 (LFA-1) function in T cells. *J. Immunol.* 157:3341–3349.
33. Zolkiewska, A., and J. Moss. 1993. Integrin $\alpha 7$ as substrate for a glycosylphosphatidylinosytol-anchored ADP-ribosyltransferase on the surface of skeletal muscle cells. *J. Biol. Chem.* 268:25273–25276.
34. Robbins, A. R., and S. I. Rennard. 1997. Biology of airway epithelial cells. *In* The Lung: Scientific Foundations, 2nd ed. R. G. Crystal, J. B. West , E. Weibel, and P. Barns, editors. Lippincott-Raven, Philadelphia. 445–457.
35. Hunninghake, G. W., J. E. Gadek, O. Karwanami, V. J. Ferrans, and R. G. Crystal. 1979. Inflammatory and immune processes in the human lung in health and disease: evaluation by bronchoalveolar lavage. *Am. J. Pathol.* 97:149–206.
36. Chu, C.-S., B. C., Trapnell, J. J. Murtagh, Jr., J. Moss, W. Dalemans, S. Jallat, A. Mercenier, A. Pavirani, J.-P. Lecoq, G. R. Cutting, W. B. Guggino, and R. G. Crystal. 1991. Variable deletion of exon 9 coding sequences in cystic fibrosis transmembrane conductance regulator gene mRNA transcripts in normal bronchial epithelium. *EMBO J.* 10:1355–1363.
37. Laemmli, U. K. 1970. Cleavage of structural proteins during the assembly of the head of bacteriophage T4. *Nature* 227:680–685.
38. Towbin, H., T. Staehelin, and J. Gordon. 1979. Electrophoretic transfer of proteins from polyacrylamide gels to nitrocellulose sheets: procedure and some applications. *Proc. Natl. Acad. Sci. USA* 76:4350–4354.
39. Rothberg, K. G., J. E. Heuser, W. C. Donzell, Y.-S. Ying, J. R. Glenney, and R. G. W. Anderson. 1992. Caveolin, a protein component of caveolae membrane coats. *Cell* 68:673–682.
40. Mojcik, C. F., D. L. Greiner, E. S. Medlock, K. L. Komschlies, and I. Goldschneider. 1988. Characterization of RT6 bearing rat lymphocytes: I. Ontogeny of the RT6 subset. *Cell. Immunol.* 114:336–346.
41. Sarkar, P., L. Crisa, U. McKeever, R. Bortell, E. Handler, J. P. Mordes, D. Waite, A. Schoenbaum, F. Haag, F. Koch-Nolte, H.-G. Thiele, D. L. Greiner, and A. A. Rossini. 1994. Loss of RT6 message and most circulating T cells after thymectomy of diabetes-prone BB rats. *Autoimmunity* 18:15–22.
42. Albelda, S. M. 1991. Endothelial and epithelial cell adhesion molecules. *Am. J. Respir. Cell Mol. Biol.* 4:195–203.
43. Sheppard, D. 1993. Identification and characterization of novel airway epithelial integrins. *Am. Rev. Respir. Dis.* 148:S38–S42.
44. Mette, S., J. Pilewski, C. Buck, and S. Albelda. 1993. Distribution of integrin cell adhesion receptors on normal bronchial epithelial cells and lung cancer cells *in vitro* and *in vivo*. *Am. J. Respir. Cell Mol. Biol.* 8:562–572.
45. Plotkowski, M. C., O. Bajolet-Laudinat, and E. Puchelle. 1993. Cellular and molecular mechanisms of bacteria adhesion to respiratory mucosa. *Eur. Respir. J.* 6:903–916.
46. Staunton, D. E., V. J. Merluzzi, R. Rothlein, R. Barton, S. D. Marlin, and T. A. Springer. 1989. A cell adhesion molecule, ICAM-1, is the major surface receptor for rhinoviruses. *Cell* 56:849–853.
47. Nelson, K. L., S. M. Raja, and J. T. Buckley. 1997. The glycosylphosphatidylinositol-anchored surface glycoprotein Thy-1 is a receptor for the channel-forming toxin aerolysin. *J. Biol. Chem.* 272:12170–12174.
48. Howard, M., J. C. Grimaldi, J. F. Bazan, F. E. Lund, L. Santos-Argumedo, R. M. E. Parkhouse, T. F. Walseth, and H. C. Lee. 1993. Formation and hydrolysis of cyclic ADP-ribose catalyzed by lymphocyte antigen CD38. *Science* 262:1056–1059.